121

Flower Pollination and Elitism Algorithms for Inversion of TDEM Data

Widodo[1*], Farkhan Raflesia [1], Susanti Alawiyah[1], Setianingsih[1], Djoko Santoso[1], Wahyudi W Parnadi[1] & Fatkhan[2]

[1]Applied Geophysics and Exploration Group, Faculty of Mining and Petroleum Engineering, Institut Teknologi Bandung, Bandung 40132, Indonesia
[2]Exploration and Engineering Seismology Research Group, Faculty of Mining and Petroleum Engineering, Institut Teknologi Bandung, Bandung 40132, Indonesia
Email: widodo@gf.itb.ac.id

Abstract Hybridization of algorithms can enhance the overall search capabilities to get the optimal solution. The aim of this study was to invert Time Domain Electromagnetic (TDEM) data using the Flower Pollination Algorithm (FPA) as a new inversion scheme technique. FPA was originally inspired by the fertilization process of flowers, in which pollen transfer grains from male flowers to female flowers. The modeling of TDEM data was done by combining the FPA and elitism (eFPA) techniques. The applicability was tested on forward modeling data and observed data in MATLAB 2017a. In testing the algorithm, we used a model from homogeneous half space to a multi-layer model using different parameters (resistivity and thickness). In addition, in the inversion process, we used field data with various starting model approaches. Based on the results of the TDEM data modeling, FPA and eFPA can both be applied as algorithmic techniques for inversion modeling of TDEM data. The eFPA technique gave better results than FPA.

Keywords: *eFPA; FPA; inversion; TDEM.*

1 Introduction

Inversion of geophysical data is essential for subsurface interpretation of processed field data responses. Inversion is physio-mathematical fitting of computed responses to measured data. Currently, inversion algorithms have been specifically developed for modeling electromagnetic data, for example, Occam inversion for EM sounding data by Constable *et al.* [1] and the Marquardt algorithm using using Singular Value Decomposition by Widodo & Saputera [2]. Since the One-dimensional (1D) inversion of EM data differs in the depth direction, it is essential in the interpretation of multidimensional models.

A TDEM field campaign is an active method that uses an artificial current source. There are two fundamental principles of TDEM measurement: Lenz's and Faraday's laws. The current injected in the transmitter produces a magnetic field.

A secondary magnetic field is generated by the eddy current when the current turns off suddenly in the conductive subsurface according to Maxwell's equations. The induced voltage of the secondary magnetic field is measured in the receiver.

According to Pellerin & Wannamaker [3], TDEM is effective in instigating a good conductor at depth, however, it is less sensitive in mapping resistivity anomalies in the low conductivity range. There are many applications of TDEM. It has been applied in hydrogeological studies [4,5], mineral exploration [6], and many more fields, ranging in scale from a few meters to several kilometers. In geological structure investigation, the TDEM technique gave good results in mapping the near surface fault structure in Mygdonian Basin [7].

The inversion model of TDEM data gives the subsurface geological parameters. To solve the inversion problem in TDEM data, many different inversion techniques can be applied, such as transient electromagnetic sounding, which uses a rapid inversion developed by Eaton and Hohmann [8], Direct inversion of TDEM data by Nekut [9], or the Laterally Constrained Inversion (LCI) algorithm by Christiansen *et al.* [10].

A hybrid variant of the FPA and elitism algorithms (eFPA) could be an alternative method to solve inversion problems of TDEM data. The simulation done by Yang [11] summarizes the FPA algorithm. The application of FPA in geophysical modeling has been conducted by Sungkono [12] to overview modeling of self-potential (SP) data and 1D vertical electrical sounding (VES) data by Raflesia & Widodo [13].

In order to test the algorithms, FPA and eFPA were applied to approximate imaging of the subsurface response of TDEM data. The forward and inversion algorithms were executed using the Matlab Programming Language. The full source code is available in Appendix A (inverse modeling), Appendix B (forward modeling), and Appendix C (Levy distribution). Improvement and modification of the script is welcomed.

2   Methods

2.1   Forward Modeling

In TDEM measurement, the vertical component magnetic field H_z is used and the time derivative of the secondary magnetic field $\left(\frac{\partial H_z}{\partial t}\right)$ can be denoted as follows[14]:

$$\frac{\partial H_z}{\partial t} = -\frac{I}{\mu_0 \sigma a^3}\left[3\mathrm{erf}(\theta a) - \frac{2}{\sqrt{\pi}}\theta a(3 + 2\theta^2 a^2)e^{-\theta^2 a^2}\right] \tag{1}$$

$$\theta = \sqrt{\frac{\mu_0 \sigma}{4t}} \tag{2}$$

$$\mathrm{erf}(x) = \frac{1}{\sqrt{\pi}} \int_{-x}^{x} e^{-t^2} dt \tag{3}$$

where a is the loop radius, I is the current, and σ is the conductivity of the earth. Due to decay of transients, the distribution of time can be distinguished into early and late times.

The calculations in the inversion program need a proper forward modeling method. We used Adaptive Born Forward Mapping [15,16] for the TDEM forward modeling. The use of this forward modeling method has also been carried out for Central Loop Time Domain Electromagnetic Inversion using the Levenberg-Marquardt algorithm. This method uses the Born series, which defines a function $(G(m))$ that changes linearly as the model (m) is updated from the reference model (m^0). The first order of the Born series is used as the $G(m)$ function approximation.

$$G(m) = G(m^0) + \int \mathcal{F}'(m^0, r)[m(r) - m^0(r)]dr \tag{4}$$

$\mathcal{F}'(m^0, r)$ is the Fréchet kernel from the function, and (r) is an unchanged variable from the Fréchet kernel. The reference model (m^0) can be expressed as:

$$G(m^0) = \int \mathcal{F}'(m^0, r)(m^0(r))dr \tag{5}$$

Thus, Equation 4 becomes:

$$G(m) = \int \mathcal{F}'(m^0, r)(m(r))dr \tag{6}$$

The Adaptive Born approximation is calculated based on the apparent conductivity of the constant half-space conductivity $\sigma_a^0 \to \sigma_a$ corresponds to the Fréchet kernel in Equation (4). Exchanging Equations (4) and (6) to equation (7) becomes

$$\sigma_a(t) = \int_0^{\infty} \mathcal{F}'(\sigma_a(t), z, t)\,(\sigma(z))dz \tag{7}$$

This equation is called Adaptive Born Forward Mapping instead of Ordinary Born Approximation. In the discrete problem, Equation 7 is formulated as:

$$\sigma_a(t_i) = \sum_{j=1}^{L} \sigma_j.\mathcal{F}_{ij} \tag{8}$$

The apparent conductivity $\sigma_a(t_i)$ at time t_i, i is i^{th} decay time, and σ_j is the conductivity model for the jth layer $(j = 1, ..., L)$.

Christensen [15] has formulated an analytic Fréchet kernel to calculate apparent conductivity, although the formula is not sufficient to approximate the conductivity response from TDEM. Therefore, approximation of the Fréchet kernel is done:

$$\mathcal{F}\left(z_j, t_i, \sigma_a(t_i)\right) = \begin{cases} \frac{z_j}{D_i}\left(2 - \frac{z_j}{D_i}\right), & \text{for } z_j \le D_i \\ \\ 1, & \text{for } z_j > D_i \end{cases} \tag{9}$$

with

$$D_i = \sqrt{\frac{c.t_i}{\mu_0 \sigma_a(t_i)}} \tag{10}$$

c is a constant of the sensitivity of the Fréchet kernel. This whole process of apparent conductivity calculation is done by using iteration. The $\mathcal{F}$ function in Equation (9) is an approximate forward mapping. The weighted sum of conductivities of each layer is denoted by:

$$\sigma_a^{k+1} = \alpha\,\sigma_a^{k+1} + (1-\alpha)\,\sigma_a^{k} \tag{11}$$

To gain stability of the calculation, single exponential smoothing is applied. Using Equation 11, the apparent conductivity from the $(k+1)^{th}$ iteration is calculated using the apparent conductivity from the kth iteration with weighting constant α.

Based on a trial-and-error process, the number of iterations that gives adequate results is 20. The transient can be estimated using Equation 1.

2.2   Inversion Method

FPA simulates the fertilization process of flowers. Fertilization can be done through self-fertilization or cross-fertilization (Figure 1). Self-fertilization is the union of female and male gametes of the same plant. It reduces the genetic diversity, while cross fertilization is the fusion of female and male gametes of different plants of the same species. Cross fertilization increases genetic diversity.
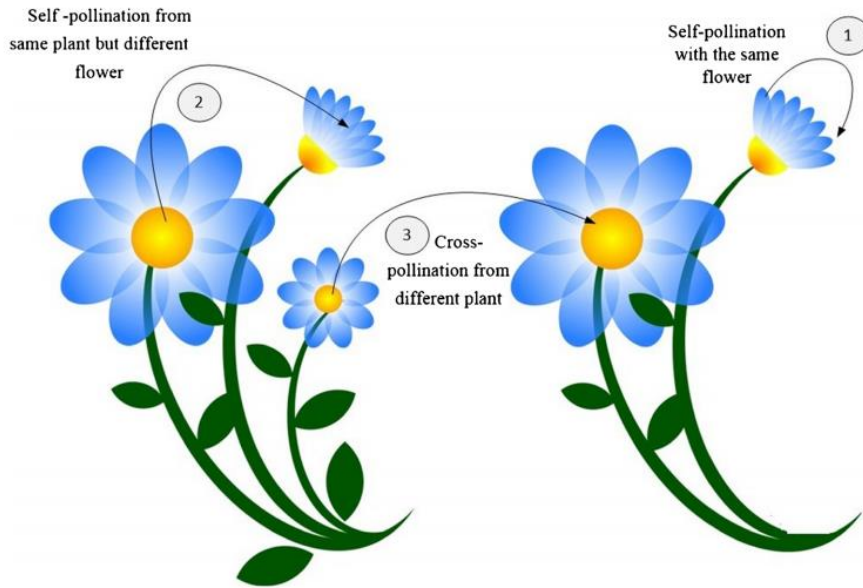
Figure 1 Flower fertilization: (1) and (2) self-fertilization, and (3) cross- fertilization from different plants [13].

The fertilization technique can be divided into global and local schemes. Global fertilization can be expressed as:

$$s_i^{t+1} = s_i^t + \alpha L(\lambda)(s_i^t - gbest) \tag{12}$$

Local fertilization can be expressed as:

$$s_i^{t+1} = s_i^t + \epsilon \ (s_j^t - s_k^t) \tag{13}$$

where, s_i^t, s_j^t, s_k^t is the fertilization of dissimilar individuals of the same species. Each index is different, $i \neq j \neq k$, while ϵ signifies a uniform distribution between 0 and 1.

Greedy selection can be expressed as [13]:

$$s_i^{t+1} = \begin{cases} s_i^{t+1} \ if \ f(s_i^{t+1}) \leq f(s_i^t) \\ s_i^t \ if \ f(s_i^{t+1}) \quad > f(s_i^t) \end{cases} \tag{14}$$

The elitism strategy produces the most suitable individuals among the candidates for selection [21]. It is a smooth method of increasing randomization, in which the best successor solutions are kept (and bad ones are replaced) to carry over to

the next iteration. The overall eFPA is summarized in Figure 2. The total population used is 100.

```
1.  Define a switch probability p ∈ [0,1];
2.  Initialize the randomly generated population within its upper and lower
    bounds;
3.  Calculate objective function of pollen using Eq. (16);
4.  Find the best solution gbest in the initial population;
5.  while abs(minRMS-maxRMS) > 10⁻¹⁰ && minRMS > 10⁻¹⁰ && iteration<1000;
6.          for i=1 : n (n indicates number of pollen);
7.              if      rand <p;
8.                      global pollination via Eq. (12);
9.              else
10.                     do local pollination via Eq. (13);
11.             end if
12.             Evaluate new solutions;
13.             Use greedy selection Eq. (14);
14.             Find the current worst solution and replace (elitism)
15.         end for
16.         Identify the present best solution gbest;
17. end while
```

Figure 2 Pseudo-code of eFPA.

The minimum function aims to obtain a response model that matches the observed data. It is denoted as the square root of the prediction error, which represents the misfit between the measured data, d_i and the model data, m, with standard deviation σ_i. The data misfit is obtained by monitoring the root mean square (RMS) error as [17]:

$$E_{RMS} = \sqrt{\frac{1}{N}\Sigma_{i=1}^{N}\left[\frac{d_i - f_i(m)}{\sigma_i}\right]^2} \, x100 \qquad (15)$$

3   Results

In order to get an appropriate model, the testing algorithms used multi-layer models. The best and worst models were created after ten FPA and eFPA runs in each study, for which the products from the number of iterations and success rates are displayed in table 1. In the calculation of TDEM data approximation, a

transmitter current of 1 Ampere was used, a loop radius of 25 m with sampling number at 20 and sampling time at $1 \, \mu s - 1 \, s$.

3.1   Synthetic Data

A synthetic model was calculated using the analytic equations from the previous sections. Three starting models were used in the forward model estimation. The first was a homogeneous layer with $100 \, \Omega m$, the second model was a more resistive layer with 100 m depth and $10000 \, \Omega m$ resistivity. The third model was a more conductive layer with 100 m depth and $1 \, \Omega m$ resistivity (Figure
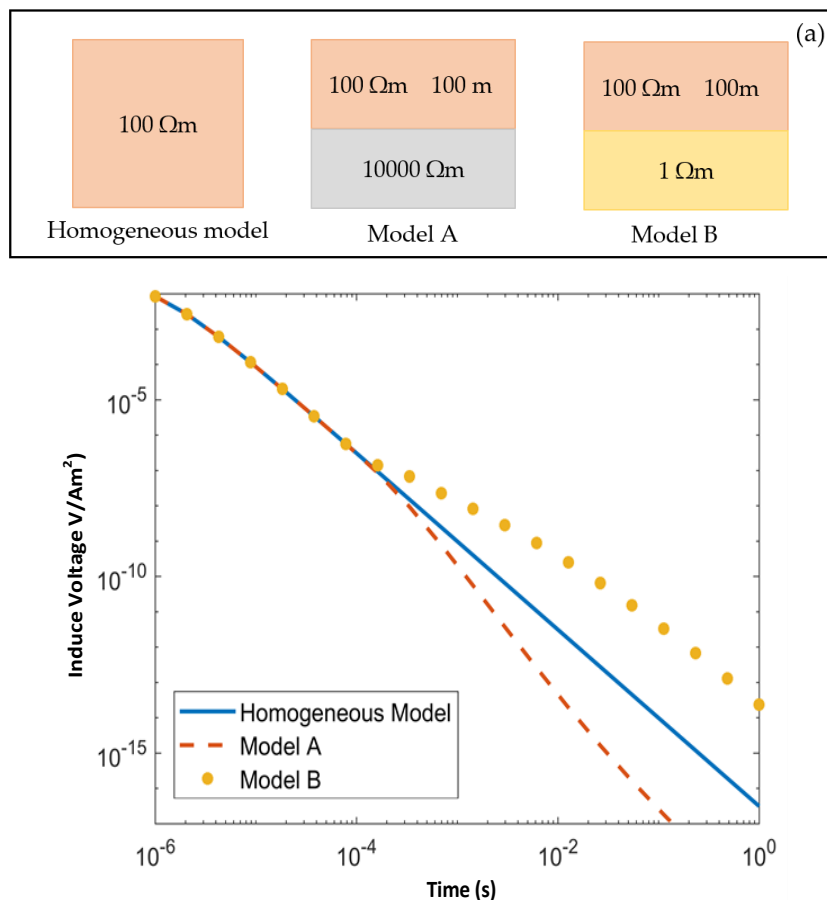

Figure 3 (a) Sketch of synthetic model, (b) TDEM response time derivative.

The transient responses of the multi-layer models are shown in Figure 3b. The homogeneous half space model gave a constant response. Initially, the transient of model A had the same feature as the transients of the homogeneous and B

models, while the curve decayed to a lower value at 10^{-4} s at the end, since the there was a resistive layer in the second layer. This lower value indicates that the decaying magnetic field was slower than the homogeneous one. The curve trend changes of the more resistive second layer shows a smoother curve compared to the less resistive layer in the second layer (Model B). The result reveals that the TEM method is capable of detecting the conductive target layer beneath the resistive overburden. Figure 4 shows the apparent resistivity results versus time.
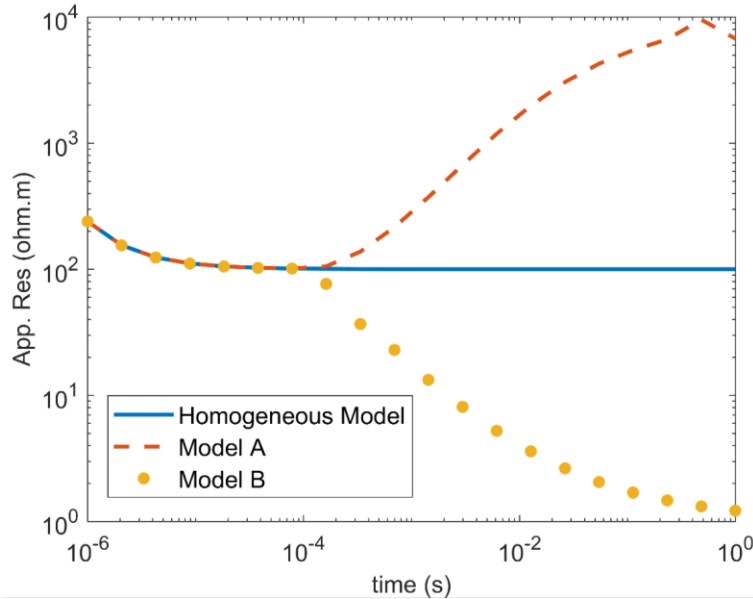

Figure 4 Curve of apparent resistivity versus time.

Table 1 Inverse results from synthetic data.

Model	Parameter	True Value	Space		FPA		eFPA	
			Min	Max	Best	Worst	Best	Worst
Homogeneous Model	ρ (Ωm)	100	1	20000	100	-	100	-
	Number of iterations				561-908		178-478	
	Number of iterations Success rate				10/10		10/10	
Model A	ρ_1 (Ωm)	100	1	20000	100.18	101.05	99.97	100.84
	ρ_2 (Ωm)	10000			10002.58	10117.14	9999.71	9961.25
	h_1 (m)	100	1	500	100.11	101.61	99.99	100.99
	Number of iterations				1000		425-701	
	Success rate				10/10		10/10	
Model B	ρ_1 (Ωm)	100	1	20000	100	-	100	-
	ρ_2 (Ωm)	1			1	-	1	-
	h_1 (m)	100	1	500	100	-	100	-
	Number of iterations				1000		457-760	
	Success rate				10/10		10/10	

Furthermore, the results of the forward modeling were inverted using FPA and eFPA to see the ability of these two algorithms in synthetic data processing. Table 1 presents the true model parameters, true value, search space, best result, worst result, number of iterations, and success rate. FPA and eFPA resulted in 10 times the global minimum solution out of 10 runs. The modeling of the inversion results from the synthetic model only shows model A because it had different values. The results of the inversion of model A can be seen in Figure 5, consisting of the true value, best and worst result of FPA and eFPA.
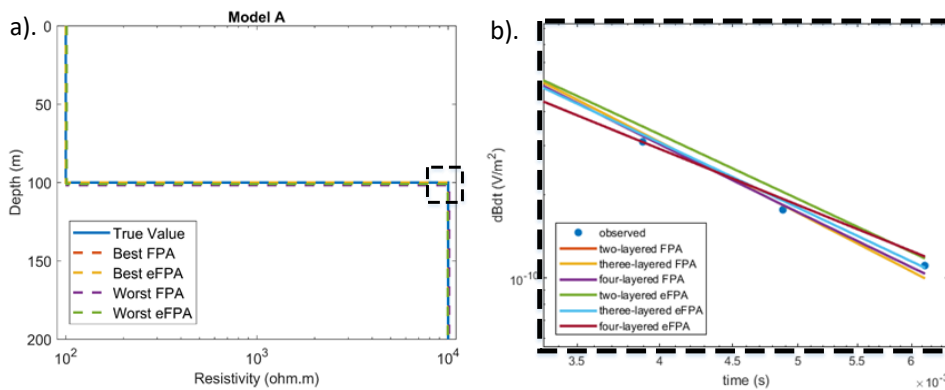

Figure 5 (a) Resistivity of model A; (b) the black dashed line indicates the magnification of Figure 5(a).

3.2   Field Data

The TDEM data were obtained in the epicenter area of the 1978 earthquake in the Volvi and Langada Lakes, Thessaloniki. This is a seismic active area, which has produced complex geological structures. The research was done by Widodo [7] using radiomagnetotelluric (RMT) and TDEM data to investigate the near-surface structure. The field campaigns were carried red using a Zonge device. Later, these data were employed in the inversion process using two, three and four-layers.

Figure 6a shows the transient of the TDEM data and its inversion results from three different starting model layers (two, three and four layers of the starting model, respectively). This technique was applied to obtain the final model. The transients gave a similar response to one another. In order to get the best model in terms of the number of layers, magnification was carried out on Figure 6a in Figure 6b. The magnified view indicates that an initial model with four layers of gave better fitting. This means that the sum of the layers of the initial models will be influenced by the final model.

Figure 7 shows inversion models of the TDEM field data for the three different initial starting models. The model resistivity of each sounding was calculated

using two, three and four layers of the initial model. The results of FPA and eFPA in the two-layered model show the same resistivity and thickness values. Meanwhile, the three- and four-layered models show different values.
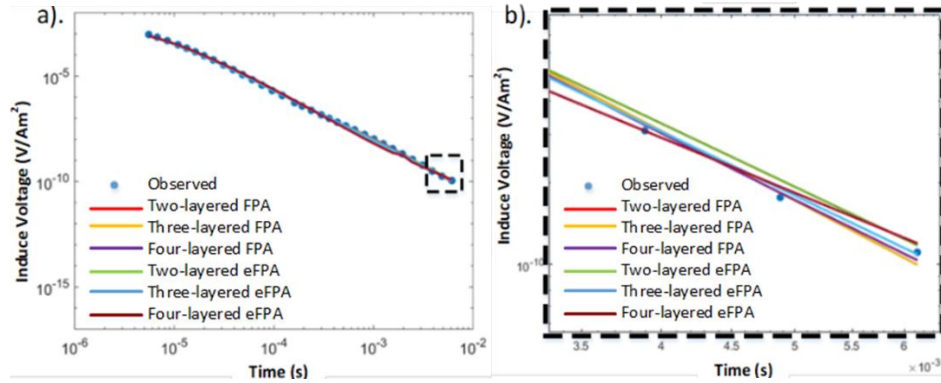

Figure 6 (a) Transient of TDEM field data using three different starting models; (b) the red square in the zoom view in Figure 6(b) shows the separated curves for each layer.
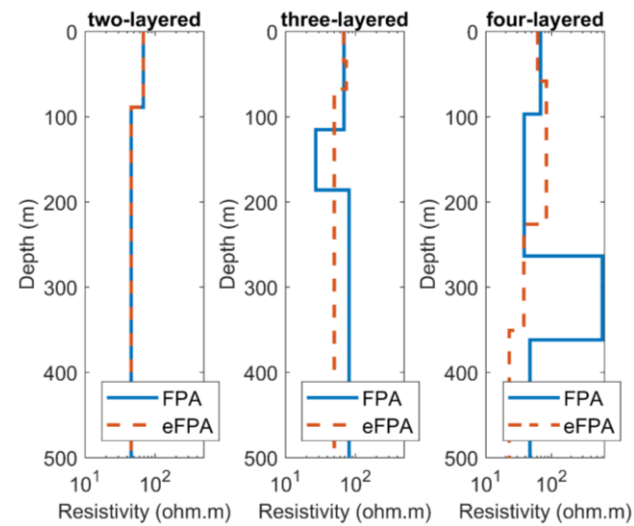

Figure 7 Resistivity model from field data

4   Discussion

Unlike the homogeneous model and model B, model A shows different values. Although it did not show the same results for the true value, the inverse results of the synthetic data from eFPA were better than FPA. In addition, the number of iterations required for eFPA was less than for FPA. FPA had more difficulty to achieve convergence, so in model A and model B the number of iterations was limited to 1000.

Figure 8a shows the comparison of the RMS errors between FPA and eFPA. FPA produced the lowest value (7.69%). The results of FPA and eFPA for the two-layered model had the same relative root mean square error values. Meanwhile, the three- and four-layered models had different values. The eFPA relative RMS error value was smaller than that of FPA for the three-layered model and the four-layered model.
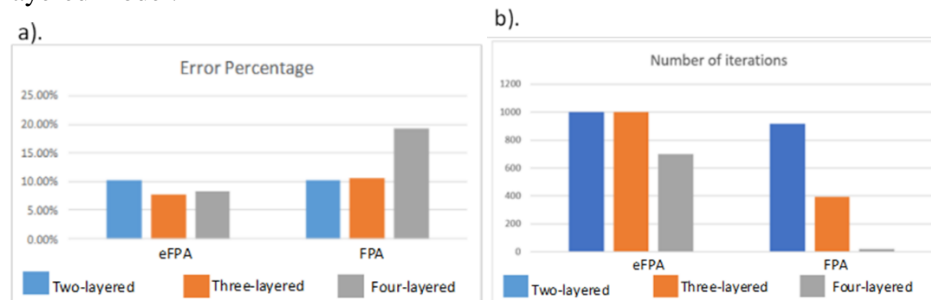

Figure 8 The performance of FPA and eFPA: (a) RMS errors of the three different starting models, (b) FPA and eFPA.

The total number of iterations for inversion modeling of the TDEM data using FPA and eFPA algorithms can be seen in Figure 8b. The algorithm of eFPA produced sufficiently competitive results against FPA's strategy, which improved the quality of the fitting data. Since eFPA enhances elitism capability, the inversion results produced better model results.

5 Conclusions

This research used a variant of the FPA and eFPA algorithms that focuses on improving the inversion of TDEM data. Algorithm testing is a time-consuming process, which can be minimized by using different search-based algorithms to meet certain coverage sizes. Hybridization of the algorithms (FPA and eFPA) gave good results in TDEM data inversion. FPA and eFPA could solve synthetic as well as field TDEM data. The provisions of the inversion process need more attention, especially for eFPA schemes.

6 Acknowledgement

7 References

[1]   Constable, S.C., Parker, R.L. & Constable, C.G., *Occam's inversion: A practical algorithm for generating smooth models for elecctromagnetic sounding data*, Geophysics, **52**, pp. 289-300, 1987.

[2]   Widodo, W. & Saputera, D. H., *Improving Levenberg-Marquardt Algorithm Inversion Result Using Singular Value Decomposition*, Earth Sci. Res. https://doi.org/10.5539/esr.v5n2p20. 2016.

[3]   Pellerin, L. & Wannamaker, P. E., *Multi-dimensional electromagnetic modelling and inversion with application to near-surface earth investigations,* Computers and Electronics in Agriculture, **46**, 71-102. 2005.

[4]   Porsani, J.L., Bortolozo, C.A., Almeida, E.R., Sobrinho, E.N.S. & Santos, T.G. (2012) *TDEM Survey in Urban Environmental for Hydrogeological Study at USP Campus in São Paulo City, Brazil*. Journal of Applied Geophysics, **76**, 102-108. https://doi.org/10.1016/j.jappgeo.2011.10.001, 2012.

[5]   Ibraheem, I. M., El-Qady, G. M. & ElGalladi, A., *Hydrogeophysical and structural investigation using VES and TDEM data: A case study at El-Nubariya–Wadi El-Natrun area, west Nile Delta Egypt NRIAG,* J. Astron. Geophysics. **5**(1), 198-215. https://doi.org/10.1016/j.nrjag.2016.04.004, 2016.

[6]   Zhenwei, G., Guoqiang, X., Jianxin, L. & Xin, W., *Electromagnetic methods for mineral exploration in China* (Review), Ore Geology Reviews, 118. https://doi.org/10.1016/j.oregeorev.2020.103357, 2020.

[7]   Widodo, Tezkan, B. & Gurk, M., *Multidimensional Interpretation of Radiomagnetotelluric and Transient Electromagnetic Data Measured in The Mygdonian Basin, Northern Greece*, Journal Engineering and Geophysics, **21**(3), 121-133, 2016.

[8]   Eaton, P.A. & Hohmann, G.W., *A rapid inversion technique for transient electromagnetic soundings*, Phys. Earth Plan. Int. 53, 384-404, 1989.

[9]   Nekut, A. G., *Direct inversion of time-domain electromagnetic data,* Geophysics, **52**, pp. 1431-1435 (15), 1987.

[10]   Christiansen, A. V., Auken, E., N, Foged & Sorensen, K.I., *Mutually and laterally constrained inversion of CVES and TEM data: A case study*, Near Surface Geophysics, 115-123, 2007.

[11]   Yang, X.S., *Flower pollination algorithm for global optimization*, in: Lecture Notes in Computer Science (Including Subseries Lecture Notes in Artificial Intelligence and Lecture Notes in Bioinformatics), htttps://doi.org/10.1007/978-3-642-32894-7_27, 2012.

[12]   Sungkono, *Robust interpretation of single and multiple self-potential anomalies via flower pollination algorithm*, Arabian Journal of Geoscience, 13, 100, 2020.

[13]   Raflesia, F. & Widodo. W., *Flower pollination algorithm for the inversion of Schlumberger sounding curve*, in: The 3rd Southeast Asian Conference on Geophysics, IOP Conf. Ser.: Earth Environ. Sci. 873 012018, 2021.

[14]   Christensen, N. B., *Imaging of Central-Loop Transient Electromagnetic Soundings*, Journal of Environment and Engineering Geophysics, 1, 53-66, 1995.

[15] Christensen, N. B., *A Generic 1-D Imaging Method for Transient Electromagnetic Data,* Geophysics, **67**, 438-447, 2002.

[16] Yogi, I.B.S., & Widodo, *Central Loop Time domain electromagnetic inversion based on Born Approximation and Lavenberg-Marquardt Algorithm*, IOP Conference Series: Earth and Environmental Science, **62**, https://aip.scitation.org/doi/abs/10.1063/1.4990901, 2017.

[17] Jackson D. D., *Interpretation of inaccurate, insufficient, and inconsistent data*, Geophysical Journal of Royal and Astronomical Society 28 97, 1972.

Appendix A

```
close all;
clear all;
clc;
tic
format long;%load data
load datahomo.dat;
dBdt=datahomo(1,:);
nl=2;                      %number of layers
nt=nl-1;
npop=100;                      %total population
prp=0.8;                      %probability
Lbr=[1 1];            %search space [lower bound resistivity]
Ubr=[20000 20000];        %search space [upper bound resistivity]
Lbt=[1];                  %search space [lower bound thickness]
Ubt=[500];
rmseror=[];
t=linspace(log10(10^-6),log(1),20);
t=10.^t;
a=25;
I=1;
for i=1:npop
  popr(i,:)=Lbr+(Ubr-Lbr).*rand(1,nl);%popr=population of resistivity
  popt(i,:)=Lbt+(Ubt-Lbt).*rand(1,nt);  %popt=population of thickness
   R=popr(i,:);
   thick=popt(i,:);
[dBdtc]=forwardloop(R,thick,t,a,I);
rms(i)=norm((dBdtc./dBdt)-1)/sqrt(length(dBdtc))*100;    %root mean square
(percentage)
end
mr=min(rms);                      %rms minimum
mrm=max(rms);                      %rms maximum
q=find(rms==mr);        %find rms minumum from population members
gRbest=popr(q,:);                      %best resistivity value
gthickbest=popt(q,:);                      %best thickness value
iteration=0;
while abs(mr-mrm) > 1E-20 && mr > 1E-9
   iteration=iteration+1;
   for i=1:npop
     if rand<prp
        n=1;
        m=nl;
        beta=1.5;
```

```matlab
        [L]=levy(n,m,beta);%levy distribution
        npopr(i,:)=popr(i,:)+(0.1.*L.*(popr(i,:)-gRbest(1,:)));      % Update the
new solutions
        npopr(i,:)=max(npopr(i,:),Lbr);      %keep resistivity always in search
space
        npopr(i,:)=min(npopr(i,:),Ubr);      %keep resistivity always in search
space
        m=nt;
        [L]=levy(n,m,beta);
        npopt(i,:)=popt(i,:)+(0.1.*L.*(popt(i,:)-gthickbest(1,:)));      % Update
the new solutions
        npopt(i,:)=max(npopt(i,:),Lbt);      %keep thickness always in search
space
        npopt(i,:)=min(npopt(i,:),Ubt);      %keep thickness always in search
space
    else
       epsilon=rand;
       JK=randperm(npop);
       npopr(i,:)=popr(i,:)+epsilon*(popr(JK(1),:)-popr(JK(2),:));
         % Check the simple limits/bounds
         npopr(i,:)=max(npopr(i,:),Lbr);
         npopr(i,:)=min(npopr(i,:),Ubr);
         npopt(i,:)=popt(i,:)+epsilon*(popt(JK(1),:)-popt(JK(2),:));
          % Check the simple limits/bounds
         npopt(i,:)=max(npopt(i,:),Lbt);
         npopt(i,:)=min(npopt(i,:),Ubt);
    end
    R=npopr(i,:);
  thick=npopt(i,:);
[dBdtc]=forwardloop(R,thick,t,a,I);
nrms=norm((dBdtc./dBdt)-1)/sqrt(length(dBdtc))*100;   %root mean square
(percentage)
   % If rms errors ok, update then
       if (nrms<=rms(i))
          popr(i,:)=npopr(i,:);
          popt(i,:)=npopt(i,:);
          rms(i)=nrms;
       end
       if nrms<mr
          gRbest=popr(i,:);
gthickbest=popt(i,:);
mr=nrms;
       end
   end
```

```
  %elitism
  mrm=max(rms);
qq=find(rms==mrm);
popr(qq(end),:)=gRbest;
popt(qq(end),:)=gthickbest;
rmseror(iteration)=mr;
end
figure(1)
plot(t,dBdt,'*r')
hold on
plot(t,dBdtc)
set(gca,'Xscale','log');
set(gca,'Yscale','log');
ylim([10^-17 10^-2]);
xlabel('time (s)');
ylabel('dBdt');
legend('obs.','cal.','location','southwest');

figure(2)
rhoplot=[0,gRbest];
thkplot=[0,cumsum(gthickbest),max(gthickbest)*1000];
stairs(rhoplot,thkplot,'--','LineWidth', 2)
ylim([0 max(gthickbest)*2]);
xlim([0.1 2000]);
set(gca,'Ydir','reverse');
set(gca,'Xscale','log');
xlabel('Resistivity (ohm.m)');
ylabel('Depth (m)');
save('dataBnaik1eFPA.txt','dBdtc', 'rmseror','gRbest','gthickbest','iteration','mr','-ascii')
```

Appendix B

```
%Function loop1d
function[dBdtc]=forwardloop(R,thick,t,a,I)
format long;
u0=4*pi*10^(-7);
c=1.2;
alpa=0.4;
depth=cumsum(thick);
C=1./R;
ac=mean(C)*ones(1,(length(t)));
for k=1:20
```

```matlab
    d=sqrt((c*t)./(ac*u0));
    z1=[0 depth];
    z2=[depth inf];
    F_t1=zeros(length(t),length(z1));
    F_t11=zeros(length(z1));
    F_t2=zeros(length(t),length(z2));
    F_t22=zeros(length(z2));
    F=zeros(length(t),length(z2));
    for i=1:length(t)
       for j=1:length(z1)
    F_t1(i,j)=d(i)-z1(j);
    F_t2(i,j)=d(i)-z2(j);
    F_t11=F_t1(i,j);
    F_t11(F_t11<0)=1;
    F_t11(F_t11>1)=(2.0-(z1(j)/d(i))).*(z1(j)/d(i));
    F_t22=F_t2(i,j);
    F_t22(F_t22<0)=1;
    F_t22(F_t22>1)=(2.0-(z2(j)/d(i))).*(z2(j)/d(i));
    F(i,j)=F_t22-F_t11;
       end
    end
        AC=C.*F;
        AC=sum(AC');
        ac=(alpa*AC)+((1-alpa)*ac);
end
TeT=((u0*ac)./(4*t)).^(0.5);
dBdtc=(u0*I./(u0*ac*(a^3))).*(3*erf(TeT*a)+(-2.*TeT.*a.*exp(-
(TeT*a).^2))./(pi^(0.5)).*(3+(2.*((TeT*a).^2))));
return
```

Appendix C

```matlab
function [L] = levy(n,m,beta)
%  Levy's flight function.
   num = gamma(1+beta)*sin(pi*beta/2); % used for Numerato
   den = gamma((1+beta)/2)*beta*2^((beta-1)/2); % used for Denominator
   sigma_u = (num/den)^(1/beta);% Standard deviation
   u = random('Normal',0,sigma_u^2,n,m);
   v = random('Normal',0,1,n,m);
   L = u./(abs(v).^(1/beta));
end
```